*Annu. Rev. Earth Planet. Sci. 1993. 21:333–73*






# THE SCALING OF IMPACT PROCESSES IN PLANETARY SCIENCES

*K. A. Holsapple*

Department of Aeronautics and Astronautics, University of Washington
FS 10, Seattle, Washington 98195

KEY WORDS: lunar crater scaling, catastrophic disruption

*"Make things as simple as possible, but no simpler."*

(Attributed to A. Einstein)

## 1. INTRODUCTION

Impact processes have shaped the solar system since its early beginnings. They are an inevitable consequence of the myriad of bodies of all sizes traveling through the same regions of space at velocities of tens of kilometers per second, and the gravitational attractions between those bodies. The results of impact processes are readily apparent in almost every image of bodies in our solar system, and are recognized as one of the most important geological processes determining the morphology of those surfaces. The observation of those surfaces is one of the most important remote sensing procedures for understanding the history and evolution of the solar system.

To make use of this unique sensing system requires an understanding and quantification of the processes of impacts. How do the observed shape and size of an impact crater depend on the underlying geology? How do they depend on the size, composition, and velocity of the impactor? What is the size distribution of the remnants of a catastrophic disruption of a body? How can one meaningfully study those processes?

This article reviews "scaling laws" for impact processes, an approach



0084–6597/93/0515–0333$02.00

used to study these questions. It presents current approaches, not an historical summary; the older approaches are only briefly mentioned in passing. The interested reader may consult the book by Melosh (1989) for mention of some of the older approaches, as well as for discussions of the mechanics of shock processes and cratering. Here the restriction of space allows only a presentation of the simplest concepts and first order theories that are the most determined; extensions to topics such as atmospheric effects, oblique impacts, time-dependent creep, and modification are only mentioned in passing.



What exactly is meant by the *scaling* of impact events, and by *scaling laws*? By *scaling* we mean to apply some relation, the *scaling law*, to predict the outcome of one event from the results of another, or to predict how the outcome depends on the problem parameters. The parameters that are different between the two events are the variables that are *scaled.* Most often these are the size scale or the velocity scale, but they can also include other parameters including a gravitational field or a material strength.

As an example, consider some easily quantified measure of the outcome of an impact such as the radius $R$ of a crater resulting from an impact into a planet of a hypervelocity body with radius $a$ and velocity $U$, of a known matcrial. The crater radius depends, among other things, on the impactor size and velocity:

$$R = f(a, U).$$

The fundamental goal of scaling studies is to measure, guess, derive, or otherwise determine the form of such a function, the scaling law, giving the dependence of the outcome of a hypervelocity impact on the size, velocity, or other conditions of the problem.

A number of questions can be raised about such scaling laws. Clearly they result from complex processes involving the balance equations of mass, momentum, and energy of continuum mechanics and the constitutive equations of the materials. The impact processes encompass the gamut of pressures—from many megabars where common solids act like fluids, to near zero where material strength or other retarding actions limit the final crater growth. Must scaling laws be power laws? Why should any such simple algebraic result be expected for such complex phenomena? If not, when are exceptions to be expected, and what form is appropriate in those cases?

Possible approaches to determining such scaling laws include experiments, analytical solutions to the governing equations, or codc calculations using those same equations. Each approach has its uses but also its deficiencies, as are now summarized.

## 1.1 *Experiment of Impacts*

Experiments are severely limited by the shortcomings of existing testing techniques. There are no well characterized techniques to launch competent compact projectiles at speeds in excess of about 8 km/sec, well below the several tens of km/sec of primary interest in the solar system. Further, only gram-sized projectiles can be launched at those speeds. Thus, one cannot test models large enough to be governed by the same physical processes as those for the ubiquitous kilometer-sized craters on solar system bodies. For meter-sized or smaller craters in geological materials the physical processes of cratering or of catastrophic disruption are governed by material strengths of the parent body. In contrast, processes responsible for kilometer-sized craters and bodies are primarily governed by gravitational forces. Experiments in the laboratory do not model the right physics for large craters. The analogy is similar, but even more severe, to attempting to predict the response of a large airplane by conducting tests on small models thrown at hand-launched speeds: The model does not have the right Reynolds number due to deficiencies in both speed and size. Large bodies do not have the simple laminar flow of small ones. For cratering, it is the *Froude number*—the ratio of dynamic to gravitational pressures—that governs the physics of large craters. Experiments typically have a Froude number several decades too large. As a consequence, laboratory experiments have limited usefulness in predicting the outcomes of impacts at planetary scales.

## 1.2 *Calculations of Impacts*

The physical laws that govern impacts are well known: the balance of mass, momentum, and energy, augmented by the constitutive laws for the materials involved. In theory one could solve those equations with appropriate numerical techniques (e.g. using the finite difference methods of the so-called hydrocodes) to determine how the outcome of an impact process is related to the defining conditions. However we lack the ability to define and correctly model the diverse material behavior over the wide range of conditions involved: Processes can begin with hundreds of megabars of pressure and millions of degrees of temperature, where all materials behave roughly as a gas, and subsequently decay to less than bars of pressure where the models of rock and soil mechanics are necessary. Even if we knew how to model this behavior in principle, we often have very imprecise knowledge of the material in question. Furthermore, from the results of a single or even multiple code runs, it is almost impossible to see the forest for the trees: It is difficult to determine fundamental dependences

of the outcome on the parameters of interest, or how they are interrelated. Consequently, while code calculations can be very instructive, one needs to know what to look for, and needs to understand the shortcomings to interpret the results.

## 1.3 *Theoretical Solutions*

If one cannot model the material behavior sufficiently to expect accurate code calculations of impact processes, then obviously one could not expect to obtain exact analytical solutions to those complicated equations. However, this does not mean that there do not exist solutions in certain limiting and idealized cases. There are such solutions, based on an approximation of the initial phases of the problem as one of a "point source." Those solutions play a significant role in determining key features of all solutions to impact problems. In fact, the primary thesis of this review will be that the existence and applicability of such solutions are the key to the understanding and derivation of scaling laws for impact phenomena. This is true even in those cases where the exact form of the solution is not obtainable: Whenever such a point-source approximation is valid certain power-law forms for scaling laws will follow.

The most well known theoretical point-source solution is for a closely related problem: the propagation in a perfect gas whole-space of the effects of the detonation of a nuclear explosion.[1] That point-source solution was determined by G. I. Taylor (1950) of the United States; and, more completely, by L. I. Sedov (1946) of the Soviet Union. It was obtained by making the approximation that the initial conditions can be described as a point source. Thus, the energy of the nuclear weapon is assumed to be instantaneously deposited in a region of zero extent. While this approximation precludes any meaningful description of the effects very near to the actual nuclear source, it gives a very accurate description for effects that are at distances large compared to the physical dimensions of the device, and at times large compared to the time of the detonation: most of the region of interest. Taylor (1950) used this solution to determine the

[1] Problems of the effects of nuclear explosions, and, to a lesser extent the effects of conventional explosives, are physically almost identical to those of hypervelocity impacts. In both cases, there is a deposition of energy and momentum in a very small initial region that subsequently is redistributed in a very large region. That distribution is accomplished by an outgoing shock that decays in time and distance. The flow field behind the shock is adiabatic. Ultimate effects and the remaining signature are determined by the physics of that flow and the physics of the material behavior as the stresses decay back to initial levels. Many of the advances in the understanding of impact physics have resulted from studies and experiments for nuclear explosions.

explosive yield[2] of the first nuclear explosion from observations on the fireball expansion.

This "air-blast" point-source solution is characterized and determined by the total energy of the explosion. The assumption that the correct measure of the point source is this energy is, however, a special assumption which is true because of the assumption of a perfect gas and a whole-space, spherically symmetric problem. For other materials, and for geometries such as half-space problems, there are still point-source approximations, but those solutions are not determined by the *energy* of the source. Instead they are determined by another single scalar measure called a "coupling parameter" by Holsapple (1981) and developed by Holsapple & Schmidt (1987). Almost all the scaling results for both explosions and for impacts are based on such point-source solutions, as will be demonstrated.



## 2. HISTORICAL APPROACHES

An introduction to current methods and a summary of past approaches is given by considering the most common and simplest scaling law: the prediction for the volume $V$ of the crater that results from the impact of a spherical body of radius $a$, velocity $U$, and mass density $\delta$ into a planet with surface gravity $g$, some strength measure $Y$ (some measure with the dimensions of stress), and mass density $\rho$.

While one can easily imagine other parameters of the problem that may affect the result, this short list suffices for the example. In fact, this is much more general than might be realized. For any material that has rate-independent behavior, all material properties include only combinations of the dimensions of stress and mass density. Thus, every additional material property can be nondimensionalized using the single strength measure $Y$ and the mass density $\rho$. Then, for scaling size and velocity *in that given material*, those additional material property groups are constant, and the discussion here holds with no loss in generality. The most general material behavior can be considered by including only one additional rate-dependent material property such as a viscosity (see Holsapple & Schmidt 1987).

It will be assumed that the planet can be considered a half-space, and that the impact is normal to the planet surface. Then the volume $V$ is determined by the listed variables:

[2] It was about 17 kton of equivalent TNT. Modern nuclear devices typically are in the megaton size. The impact of the bolide of the presumed KT event, with a diameter of perhaps 10 km at 20 km/sec, would have an energy equivalent to over $10^5$ gigatons of TNT. That is a factor of $10^4$ times the total yield of all nuclear weapons ever built by mankind.

$$V = f[\{a, U, \delta\}, \{\rho, Y\}, g] \tag{1}$$

with a grouping of the variables into those defining the impactor, those defining the material of the planet, and the surface gravity of the planet.

Dimensional analysis is the primary tool used to derive scaling theories. In the case of the Equation (1), there are seven parameters, with the three independent dimensions of mass, length, and time. Therefore, there is a simpler relation among four (seven minus three) dimensionless combinations (groups). The choice of these groups is not unique, and all results are independent of the forms chosen. The form chosen uses the mass $m$ of the impactor as well as its radius:

$$\frac{\rho V}{m} = f\left[\frac{ga}{U^2}, \frac{Y}{\rho U^2}, \frac{\rho}{\delta}\right], \quad m = \frac{4\pi}{3}\delta a^3 \tag{2}$$

The dimensionless groups in these relations can be interpreted. On the left is the ratio of the mass of material of the crater to that of the impactor. This is called the *cratering efficiency*, and is often denoted by $\pi_V$. The first term inside the function is, to within a numerical factor, the ratio of a lithostatic pressure $\rho ga$ at a characteristic depth equal to one projectile radius to the initial dynamic pressure $\rho U^2$ generated by the impactor. This is the inverse of the definition of the Froude number. It has traditionally[3] been denoted as $\pi_2$ (see, for example, Holsapple & Schmidt 1982). Its presence in (2) allows the cratering efficiency to vary (it decreases) as either the size of the impactor, or the gravity level increases. The second term in the function is the ratio of a crustal material strength to the initial dynamic pressure; it will be denoted as $\pi_3$. Finally, the last term is the ratio of the mass densities.

If one could completely determine this function by calculation or experiment then the scaling problem would be solved. However, as stated, neither is practical, so further simplifications are pursued.

The ratio of the mass densities is usually about unity (and, since there is no problem matching its value in experiments, it will be omitted for now and the dependence on the remaining variables studied). Strengths of geological materials range from less than bars for soils to more than 10s of kbar for small samples of competent rocks. However, this latter value

[3] In many previous cases it has been plotted as $3.22ga/U^2$, where the factor is twice the cube root of $4\pi/3$. This makes it consistent with explosive results, where the specific energy of the device is equivalent to $1/2U^2$ and the $4\pi/3$ factor arises when the cube root of $m/\delta$ is replaced by the radius $a$.

is not characteristic of the large-scale geologies of planetary surfaces because of the presence of faults and cracks. Thus, the effective values of crustal strengths range from less than 1 bar to 1 kbar. In comparison, on the Earth's surface the lithostatic pressure is about 0.3 bars for each meter of depth. These values lead to a natural partition between two size scales of impacts, one appropriate for "strength-dominated" and one for "gravity-dominated" cratering, depending on the size of the event.

If, for the Earth, the impactor is smaller than about meter-sized, then the strength of a soil surface is large compared to the lithostatic pressure and the lithostatic pressure can be ignored. (The maximum size for which strength is large compared to the gravitational pressures depends linearly on the crustal strength and inversely on the surface gravity of a planet.) In this case, Equation (2) becomes

$$\frac{\rho V}{m} = \bar{f}\left[\frac{Y}{\rho U^2}\right]. \tag{3}$$

Consequently, in this "strength regime" the volume of the crater increases linearly with the volume of the impactor, its mass, and—at constant velocity only—its energy. By the same argument, any crater linear dimension such as its diameter $d$ increases linearly with the cube root of the impactor volume and mass: i.e. with the projectile radius. Such a dependence is often called "cube-root" scaling, or "strength scaling." The dependence on the velocity, however, remains undetermined. In principle, experiments to determine the velocity dependence are possible: One can shoot a projectile (at up to 8 km/sec) into appropriate specimens. However, one must then extrapolate to velocities of several 10s of km/sec. Because this extrapolation begins from processes that have little or no melt and extends to processes that have significant melt and vapor near the impact point, the extrapolation is very uncertain. Most experiments of impacts are performed in this strength-dominated regime and at relatively low velocities, and, as a consequence, give limited information on the majority of cases of primary interest.

At the other extreme, when the impactor is kilometer-sized or larger, then the crustal strength is small compared to the lithostatic pressure term. This defines the "gravity regime" for which Equation (2) becomes

$$\frac{\rho V}{m} = \bar{f}\left[\frac{ga}{U^2}\right]. \tag{4}$$

Thus, in the gravity regime the crater volume is not proportional to the impactor volume or mass, nor is it necessarily proportional to its kinetic

energy.[4] The dependence on either the size or the velocity, which are related in a particular way, must be determined by experiment or by numerical calculation.

Consider experiments in this case. Problems of interest have variations of the velocity of about a decade, in projectile size of about five decades [spanning laboratory diameters (cm) to solar system diameters (10 km)], and in gravities ranging from near zero to a decade larger than the Earth's. Then the range of inverse Froude numbers of interest in (4) is about $10^{-6}$ to $10^{-2}$, a four decade range. (For very small gravity such as on smaller asteroids, the strength regime governs all impacts.)

To determine the function for increasing $\pi_2$, one could perform experiments at a fixed velocity at increasing projectile diameter or one could decrease the velocity at fixed size. However, for velocities below a few km/sec, the impacts are no longer hypervelocity ones; different physics controls the process and additional parameters will occur in (4). Experiments should be at velocities as large as possible. Then the largest possible value for experiments at Earth's gravity and for cm-sized projectiles has an inverse Froude number of about $10^{-6}$, and experiments in the actual regime of interest are not feasible.

Only one possibility for experiments in the gravity regime for common soils exists: These involve increasing the gravitational forces. The technique was begun in the late 1970s, both for explosive cratering and for hypervelocity impact cratering, by Schmidt (1977, 1980) and later developed by Schmidt & Holsapple (1978a,b, 1980) who performed experiments on a large geotechnical centrifuge, with gravity increased by a factor approaching three decades. Froude numbers in the gravity regime were thus obtained.

The first experiments of this type were performed in a dry sand. In such cases, the cohesive strength of the material is essentially zero, so that the gravity regime also extends back to much smaller inverse Froude numbers. The results obtained from those experiments were very revealing, and provided the first clues that led to much of the recent theory on scaling. Some results of Schmidt & Holsapple (1980) are reproduced here as Figure 1. (These experiments were for explosive cratering, rather than impact. In this case, the parameters used are the explosive energy per unit mass $Q$, equivalent to $U^2/2$ for an impact, and the explosive mass $W$, equivalent to the mass $m$ of the impactor.) While the functional form shown in (4)

[4] It is interesting to note that, until the past decade, researchers of nuclear weapons effects always assumed that the strength regime and cube-root scaling, as in Equation (3), applied to the hundred of meter diameter craters produced by nuclear weapons in the megaton yield range. More recently, they have recognized the deficiency of such an assumption for large nuclear craters also. Schmidt et al (1986) give nuclear and conventional explosive cratering estimates using the gravity scaling.

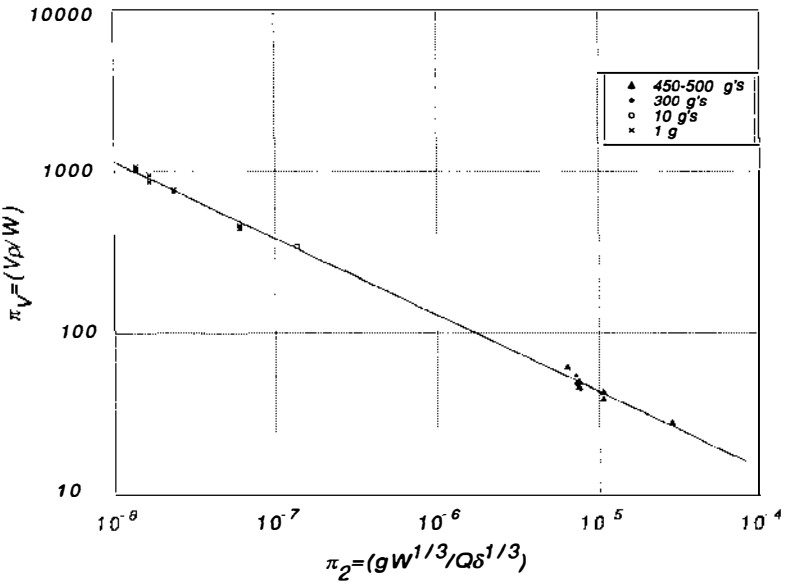


*Figure 1* Explosive cratering results in a dry sand at normal and elevated gravity. The power-law fit extends at least four decades in the gravity-scaled size parameter, giving decreasing cratering efficiency with either increasing explosive size or increasing gravity.

predicts that there should be some smooth relation between the groups plotted on the ordinate and abscissa of this figure, the data show a very particular functional form: an exact power law over almost four decades of the abscissa, with a power exponent of $-0.47$. This power-law form is not predicted by the dimensional analysis leading to (4).

A similar result existed in the literature for impacts into dry sand. Gault & Wedekind (1977) report on a series of one-*g* and less than one-*g* experiments at fixed energy. (The interest was in lunar craters. However, the occurrence of the factor *ga* in the Froude number shows that using a 1 cm projectile at Earth's gravity to simulate, for example, the effect of a 10 m bolide striking the Moon with a gravity 1/6 of that of the Earth requires an *increased* gravity by a factor of 167, not a reduced gravity.) Separately, Oberbeck (1977) reported a series of variable energy impacts at one-*g*. Schmidt (1980) extended those results to larger inverse Froude numbers by adapting the centrifuge testing methods to impact problems. When combined and plotted as in Figure 1, a power law is observed with a slope of approximately $-0.50$, as reported by Schmidt (1980). The question was, why were these results all exactly power laws?

Described in the literature was one approach that predicted a power law. An appealing assumption, consistent with the results for the related air-blast problem and with the older literature on explosive cratering, is that the dependence on the impactor size and velocity is on its *kinetic energy* only, irrespective of its separate size and velocity. In this case (1) becomes

$$V = f[\{mU^2\}, \{\rho, Y\}, g]. \tag{5a}$$

The dimensional analysis now leads to a restricted form of (2):

$$\frac{\rho V}{m}\left[\frac{ga}{U^2}\right]^{3/4} = \bar{f}\left\{\left(\frac{Y}{\rho U^2}\right)\left[\frac{ga}{U^2}\right]^{-3/4}\right\}, \tag{5b}$$

which for the strength regime gives a special case of (3):

$$\frac{\rho V}{m} \propto \left(\frac{Y}{\rho U^2}\right)^{-1}, \tag{5c}$$

and for the gravity regime reduces to a special case of (4):

$$\frac{\rho V}{m} \propto \left[\frac{ga}{U^2}\right]^{-3/4}. \tag{5d}$$

In the historical scaling approaches, it was assumed a priori that the energy of the impactor determined the resulting crater size, so that (5c) applied. For example, Shoemaker (1963) used this cube-root law and scaled from a relatively deeply buried nuclear event "Teapot Ess" to estimate the energy of the meteorite that created Meteor Crater in Arizona. This approach was adopted from the explosive cratering literature, in which the form (5c) was introduced by Lampson (1946) in studies of craters from explosions of up to about one ton explosive mass—cases predominantly within the strength regime. In addition, it should be noted that all common chemical explosions have essentially the same specific energy (about $4.2 \times 10^{10}$ ergs/gm), which is equivalent to a single impact velocity of 2.9 km/sec. Therefore, it was easy to overlook the possibility that there might be a separate specific energy dependence in the data, i.e. to overlook the important difference between (5c) and the more general (3). (Nuclear weapons have specific energies over 6 decades higher.)

In the gravity regime, this "energy-scaling" assumption predicts that there should be a power law, but with exponent $-3/4$ (Equation 5d)—substantially different from the observed slopes of about $-1/2$. Since a linear crater dimension would then vary as the $-1/4$ power of the energy,

this is called "quarter-root" scaling: It is the consequence of the energy scaling assumption in the gravity regime.

In the literature of the 1960s pertaining to micrometeorite impacts into the metals of spacecraft, along with those who thought that the energy of an impactor should govern the results, was an opposing camp who promoted the *momentum* of the impactor as its definitive measure. [Later, Holsapple & Schmidt (1982) showed that these are the two limits on possible scaling.] If this momentum, equal to $mU$, is used in (5a), then one again gets a power law as in (5c) for the gravity regime, but now with a power of $-3/7$. Although closer to the observed results for dry sand, the magnitude of the exponent ($-3/7$) is *below* that observed.

At about the same time another important experimental result was reported by Gault (1978) for the maximum transient crater formed by hypervelocity impacts into water. In reporting his results, he again assumed a dependence only on the energy of the impactor and reported that a plot of maximum instantaneous volume versus energy gave the exponent of $-0.75$ as appropriate for energy scaling. However, the data were reinterpreted using the more general dimensionless groups of (4) by Holsapple & Schmidt (1982) who concluded that a substantially better fit was a power law as in (5c) but with an exponent of $-0.65$.

There were interesting experiments reported at the turn of the century by Worthington & Cole (1897) and Worthington (1908) for (maximum transient) craters formed in water by simply dropping rigid balls into a container of water. The impact velocities were in the range of 1 to 20 m/sec. Theirs and other more recent data were examined by Holsapple & Schmidt (1982) and a fascinating result was observed. The best fit power-law curve through the Gault (1978) data (where the velocities of impact were 6 km/sec) extrapolated to over 6 decades in the Froude number goes right through the center of the low speed data. A power law with exponent of $-0.65$ holds for over 9 decades of Froude number for impacts into water.

Figure 2 shows these data, as reproduced from Holsapple & Schmidt (1982). Again, there was very powerful experimental evidence for power-law scaling laws for cratering efficiency over multiple decades of the gravity-scaled size.[5]

These observations, as well as others, led to the approach given by Holsapple (1981, 1983) and Holsapple & Schmidt (1987). It was recognized that the assumption that the kinetic energy of the impactor governed all subsequent results is in fact equivalent to a point-source assumption, where

[5] The simple water-drop experiments using 1 cm balls with 10 m/sec impact velocity have the same Froude number as a 10 km/sec impact into Earth's ocean of a 10 km bolide!

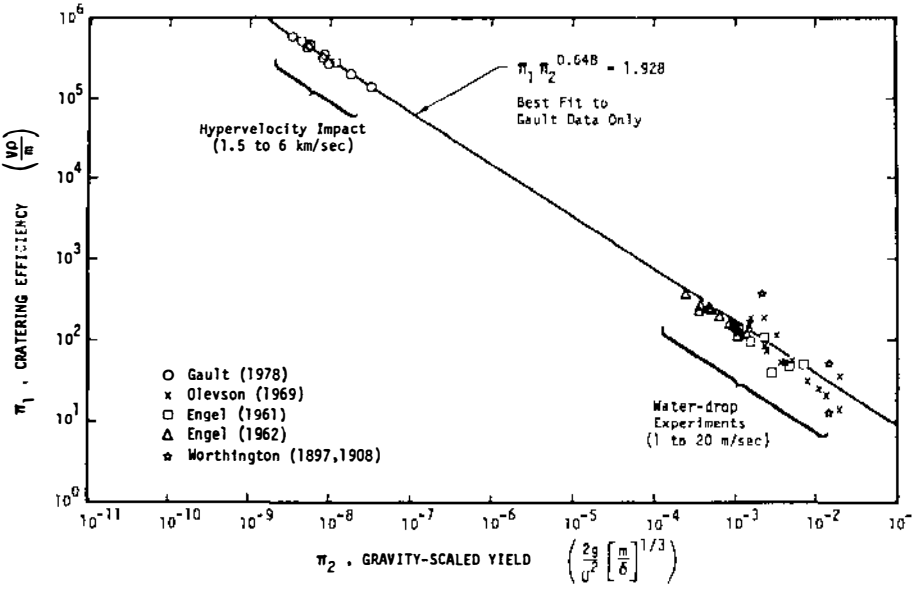


*Figure 2* Data for cratering in water for velocities from 1 m/sec to 6 km/sec. A single power-law fit through the hypervelocity data goes right through the low speed data. Thus, a single power-law fit holds for over 8 decades of impactor radius (24 decades of mass), 4 decades in impact velocity, and 8 decades in gravity.

the measure of the impactor is $1/2mU^2$. It is convenient to take a cube root of this, to use the impactor radius, and to drop a numerical factor to get the measure

$$C = \delta^{1/3} a U^{2/3}. \tag{6a}$$

Alternatively, the assumption that the *momentum* dominates all results is equivalent to a different point-source assumption, with the measure

$$C = \delta^{1/3} a U^{1/3}. \tag{6b}$$

While the only well-known actual point-source solution was that for the spherical air-blast problem (for which it was indeed the energy that governed), there were other point-source solutions in related literature where other measures governed. The book by Barenblatt (1979) presents a detailed exposition of a class of problems in mechanics termed "self-similar of the second kind." In distinction to those he calls "of the first kind," those of the second kind are governed by point-source approximations for which certain exponents governing those solutions are not known a priori, but depend on the parameters of the problem and are

determined in the course of the solution. A study of those point-source problems and the nature of their solutions leads to the current scaling approaches.

## 3. POINT-SOURCE SOLUTIONS

In an impact problem, one starts with the assumption that the impactor size $a$, velocity $U$, and mass density $\delta$ each affect the outcome. Those measures of the impactor give a size scale $a$, a velocity scale $U$, a time scale $\tau = a/U$, and a mass scale $\delta a^3$. Clearly those three separate measures can separately affect certain aspects of the results. For example, the initial pressure generated for sufficiently high-speed impacts is proportional to the square of the velocity. The amount of melt or vapor may be determined by the velocity and the mass of the projectile. The time to transfer the energy and momentum of the projectile into the target and for the shock to traverse the projectile is proportional to the time scale.

On the other hand, it seems entirely reasonable that these scales can only affect the solution very near to the impact point. For phenomena at a distance of many projectile radii, and at times of many scale times, how much can the details near the impact source affect the results? How much can they affect the final crater volume? Can the source region be approximated as a point source? In an early paper, Rae (1970) assumes so, and considers some aspects of the shock propagation of point-source solutions to the impact problem.

In mathematics a point-source solution is introduced as a limit. A problem very similar to the nuclear air-blast problem mentioned previously provides an example. Consider an infinite region filled with a perfect gas of initial mass density $\rho_0$, where at the initial instant there is a high pressure spherically symmetric "source" region of radius $a$ and pressure $P_1$, but where the rest of the infinite region is initially at some low pressure $P_0$. The sole material property of a perfect gas is the perfect gas constant $\gamma$. The initial pressure and size define the initial energy of the problem (internal rather than kinetic in this case),

$$E_1 = \frac{4\pi}{3} \frac{P_1}{\gamma - 1} a^3. \tag{7}$$

Because of that initial spatially discontinuous state, there will be a spherical shock generated which propagates outward with time. Denote by $R$ the position of that shock and by $P_f$ the pressure at the shock which are functions of time $t$. Behind the shock the pressure $p$ will be a function

of radial position $r$ and time $t$. All depend on the problem parameters. Thus

$$p = p(r, t, a, P_1, P_0, \rho_0, \gamma) \tag{8a}$$

$$R = R(t, a, P_1, P_0, \rho_0, \gamma) \tag{8b}$$

$$P_f = F(t, a, P_1, P_0, \rho_0, \gamma). \tag{8c}$$

These can be written in a nondimensional form as

$$\frac{p}{P_1} = f\left(\frac{r}{a}, \frac{t}{t_1}, \frac{P_0}{P_1}\right) \tag{9a}$$

$$\frac{R}{a} = f\left(\frac{t}{t_1}, \frac{P_0}{P_1}\right) \tag{9b}$$

$$\frac{P_f}{P_1} = f\left(\frac{t}{t_1}, \frac{P_0}{P_1}\right), \tag{9c}$$

where the dependence on the dimensionless perfect gas constant is understood, and the source region length scale $a$, and a time scale defined as $t_1 = a\sqrt{\rho_0/P_1}$ are used to nondimensionalize. Here we consider only the "strong-shock" regime, where all pressures are very large compared to the pressure $P_0$. Then the pressure ratio $P_0/P_1$ can be dropped from further consideration.

For the asymptotic form of these relations when the time $t$ and distance $r$ are large compared to the source scales, the ratios $r/a$ and $t/t_1$ are large. These ratios also become large in a different limit as the source size and time scale become small, which is the limit leading to the definition of a point source. A point-source problem is then a limit of problems where the initial size scale $a$ and the time scale $t_1$ go to zero, but where the initial pressure $P_1$ becomes infinite in some (as yet) undefined way. The fundamental question is whether such a limit exists in a nontrivial way (not become infinite or identically zero); and, if so, how the initial pressure must grow to infinity.

An answer to this last question can be given. Suppose that in the limit the pressure $P_1$ and the source size $a$ vary in some particular way:

$$\lim_{a \to 0} (P_1 a^\beta) \to \text{constant} \tag{10}$$

for some particular positive value of the exponent $\beta$. Then in that limit the sole remaining measure of the source region is the single scalar $P_1 a^\beta$ or, by taking a root, $aP_1^{1/\beta}$. In this case the three variables remaining in (9a) can be recombined into two as

$$\frac{p}{P_1}\left(\frac{r}{a}\right)^{\beta} = f\left[\frac{t}{t_1}\left(\frac{r}{a}\right)^{-(\beta+2)/2}\right], \tag{11}$$

which gives a form that does not become indeterminate in the limit, as a consequence of (10) and because of the definition of the time scale.

Thus, point-source limits may exist when some combined measure of the initial pressure and size is fixed in the limit process.[6] That measure determines all characteristics of the point-source limit.[7] In the limit, Equations (9b) and (9c) can also be recombined to become

$$\frac{R}{a}\left(\frac{t}{t_1}\right)^{-2/(\beta+2)} = \text{constant} \tag{12a}$$

$$\frac{P_f}{P_1}\left(\frac{t}{t_1}\right)^{2\beta/(2+\beta)} = \text{constant} \tag{12b}$$

showing that in this point-source limit the shock front moves outward as a power law, with power $2/(2+\beta)$ and the shock pressure decays with time to the power $-2\beta/(2+\beta)$. The remaining question is, of course, what is the correct value for the exponent $\beta$? While one might suppose that the initial energy given in (7) should govern the solution, such an hypothesis (which is in fact correct in this particular spherical, perfect gas case) must be proved. Why could not some other combination of the pressure and size govern?

Assuming that the energy governs the solution, then the total initial energy in (7) must be held constant in the limit process defined in (10), and from (7) it is seen that $\beta = 3$. Then the shock moves outward in time with the power of 2/5 and the pressure decays in time as the power of $-6/5$. Taken together, these imply that the pressure decays with distance to the power of $-3$. These results are well known for spherical air-blast problems.

How does one prove the existence of such a limit? How does one obtain the unknown exponent of the source measure? Barenblatt (1979) shows how to determine the unknown exponent for certain examples of self-similar, point-source problems. Generally, it is determined as an eigenvalue

[6] The proof of the actual existence of such a limit must be done on a case-by-case basis.

[7] The relation (11) is an example of what are called *self-similar solutions* in the study of solutions to partial differential equations in mathematics. Thus, a point-source limit (in the strong shock regime) is by necessity self-similar. At sufficiently large times, the pressures will decay to where the atmospheric pressure in front of the shock can no longer be ignored. The solution still arises from an initial point source, but it is no longer self-similar. Therefore, while self-similar solutions are point-source solutions, the converse is not true: Point source solutions need not be self-similar, and generally will not be in the far field.

from a nonlinear ordinary differential equation of first order that must satisfy two end conditions. Fortunately, the theoretical determination of the exponent is not needed here; it suffices to know the general form that such point-source solutions must take. The existence of a single scalar measure of the form in (10) is sufficient to determine the form of scaling laws, and relations between different aspects of the same problem. We now return to the impact problem and derive such forms.

## 4. SCALING LAWS FOR CRATERING

It has been shown above how point-source solutions determine power-law scaling laws in terms of some single combined measure of the source. The converse is also true: Since any power-law form has a combined single measure, that form implies a point-source measure. Based on that, Holsapple (1981) considered a single measure

$$C = aU^{\mu}\delta^{\nu} \tag{13}$$

assumed to measure the results in the far field of the impact of a bolide with radius $a$, velocity $U$, and mass density $\delta$. This same approach was used by Dienes & Walsh (1970) for impacts into metal targets; they called the approach "late-stage equivalence." The exponents $\mu$ and $\nu$ remain undetermined for now, but special cases can be noted. If the impactor kinetic energy is the correct measure, as has been assumed for energy scaling in the past (this turns out never to be exactly correct for the problems of interest here), then $\mu = 2/3$ and $\nu = 1/3$. For the momentum assumption, $\mu = 1/3$ and $\nu = 1/3$.

The terminology "coupling parameter" is used since it is the sole measure of the coupling of the energy and momentum of the impactor into the planetary surface. It must then determine all subsequent scaling laws for all phenomena appropriately determined by the far-field solution.[8] This coupling parameter is determined by the two exponents $\mu$ and $\nu$. Therefore, all scaling laws of impact processes will involve those exponents in some specific way. Several of the more important examples of the development of those scaling laws are presented here. The reader can refer to Holsapple (1987) and Holsapple & Schmidt (1987) for more complete results and tables of scaling forms.

[8] It is not always clear which effects are sufficiently far from the source to be included. However, code calculations (see Holsapple 1982, 1984) have routinely showed that the solutions approach that of the point-source solution for a distance within one to two impactor radii. (See also O'Keefe & Ahrens 1992b.) For a feature such as the amount of melt or vapor produced, it is more likely that this measure should not be used but instead scaling based on the near-field solution would be better.

## 4.1 *Crater Volume*

When there is this single measure of the impactor, relation (1) for volume scaling takes the special form

$$V = f[aU^{\mu}\delta^{\nu}, \rho, Y, g]. \tag{14}$$

[Holsapple & Schmidt (1987) also included a dependence on a material viscosity, which is useful for cratering in viscous materials, but is probably not required for the majority of applications. The interested reader can consult that reference for the more general results.]

To do a dimensional analysis one must recognize that the dimensions of the coupling parameter depend on the two exponents $\mu$ and $\nu$. There are now only two (five minus three) dimensionless groups. Two alternative useful forms obtained are

$$\frac{\rho V}{m}\left(\frac{Y}{\rho U^2}\right)^{3\mu/2}\left(\frac{\rho}{\delta}\right)^{3\nu-1} = F\left[\frac{ga}{U^2}\left(\frac{\rho U^2}{Y}\right)^{(2-\mu)/2}\left(\frac{\rho}{\delta}\right)^{\nu}\right] \tag{15a}$$

$$\frac{\rho V}{m}\left[\frac{ga}{U^2}\right]^{3\mu/(2+\mu)}\left(\frac{\rho}{\delta}\right)^{(6\nu-2-\mu)/(2+\mu)} = G\left\{\frac{Y}{\rho U^2}\left[\frac{ga}{U^2}\right]^{-2/(2+\mu)}\left(\frac{\rho}{\delta}\right)^{2\nu/(2+\mu)}\right\}. \tag{15b}$$

These forms may look complicated, but the functions now have a *single* variable. They give explicit results in both the strength and the gravity regime limits. In the strength regime gravity can be ignored; the function of the right of (15a) is a constant $F[0]$ so that

$$V \propto \frac{m}{\rho}\left(\frac{\rho U^2}{Y}\right)^{3\mu/2}\left(\frac{\rho}{\delta}\right)^{1-3\nu}. \tag{16a}$$

Similarly, ignoring the strength in (15b) gives for the gravity regime

$$V \propto \frac{m}{\rho}\left[\frac{ga}{U^2}\right]^{-3\mu/(2+\mu)}\left(\frac{\rho}{\delta}\right)^{(2+\mu-6\nu)/(2+\mu)}. \tag{16b}$$

Based on some plausible hypotheses Holsapple & Schmidt (1982) showed that the momentum scaling and the energy scaling give the upper and lower bounds on the scaling exponent $\mu$. Thus, $1/3 \leq \mu \leq 2/3$. For both limit cases the exponent $\nu$ is 1/3, so this is a likely general value also. Since for all cases of interest the mass density ratio does not deviate from unity by more than a factor of three or so, the terms with that ratio are of the order of unity, and will often be omitted.

All of these results can be illustrated as shown schematically in Figure

3, which shows the cratering efficiency $\pi_V$ versus the gravity-scaled size parameter $\pi_2$ as it would appear on a log-log plot. In the strength regime, the cratering efficiency is constant for increasing impactor size but depends on the velocity. In the gravity regime, the cratering efficiency decreases with increasing impactor size as shown. The exponent of that decrease has been often denoted by $-\alpha$; comparison with (16b) yields

$$\alpha = \frac{3\mu}{2+\mu}. \tag{17}$$

The limits on $\alpha$ are 3/7 to 3/4.

Experiments in an alluvial soil on a centrifuge (Holsapple & Schmidt 1979) for explosions have indicated that the transition between the strength and the gravity regimes typically spans about two decades in the $\pi_2$ parameter, over which the gravity lithostatic pressure ranges from about 1/10 the strength to 10 times the strength. Following the approach of Holsapple & Schmidt (1979) a convenient empirical smoothing function to span the transition can be given as

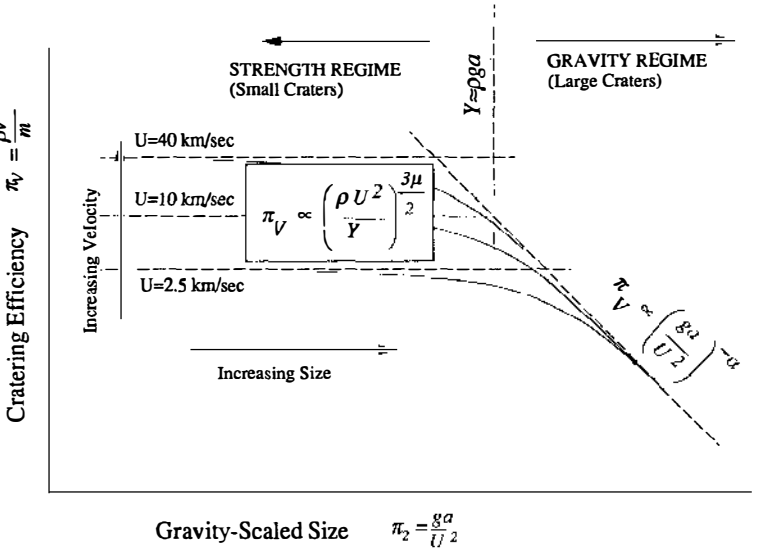


*Figure 3* The regimes of cratering for a material with strength. In the strength regime the cratering efficiency depends on the impact velocity, but is independent of gravity-scaled size. For increasing size at a fixed velocity, there is a transition to the gravity regime in which the cratering efficiency has a power law decrease with increasing size. Most experiments in geological materials are by necessity in the strength regime.

$$\pi_V = K_1\left\{\pi_2\left(\frac{\rho}{\delta}\right)^{(6\nu-2-\mu)/3\mu} + \left[K_2\pi_3\left(\frac{\rho}{\delta}\right)^{(6\nu-2)/3\mu}\right]^{(2+\mu)/2}\right\}^{-3\mu/(2+\mu)}$$

$$\pi_V = \frac{\rho V}{m}, \quad \pi_2 = \frac{ga}{U^2}, \quad \pi_3 = \frac{Y}{\rho U^2}, \tag{18}$$

where the definitions of the dimensionless groups for the cratering efficiency, the gravity-scaled size, and the strength group are again indicated. This has the correct limits in both regimes. The two constants $K_1$ and $K_2$ as well as the exponents $\mu$ and $\nu$ can be chosen to match the results in each of the gravity regime and the strength regime. Henceforth, it will be assumed that $\nu = 1/3$ in all cases, which simplifies the results. [Holsapple & Schmidt (1979) omitted the power on the strength term since it was not recognized that the exponent in the strength regime and that in the gravity regime must both be determined by the common exponent of the point-source solution. Holsapple & Schmidt (1987) later gave a correct form.]

The material strength $Y$ occurs in the numerator of the second term as the product $K_2Y$ which is then determined from cratering experiments in the strength regime. One can take $K_2$ equal to unity and then determine an effective strength $\bar{Y}$ to match the strength-dominated, small-scale cratering results. This approach will be used. The notation $\bar{\pi}_3$ is used to denote that choice. Then Equation (19) gets somewhat simpler:

$$\pi_V = K_1\left[\pi_2\left(\frac{\delta}{\rho}\right)^{1/3} + \bar{\pi}_3^{(2+\mu)/2}\right]^{-3\mu/(2+\mu)}. \tag{19}$$

This equation is then used for the scaling of crater volume for all materials. The transition between the two limits occurs when the two terms inside the brackets are equal. This occurs when the gravity-scaled size $\pi_2$ parameter defined above is equal to $(\bar{Y}/\rho U^2)^{(2+\mu)/2}$.

Schmidt & Housen (1987) present estimates of this form[9] for wet and dry soils and for water. Additionally, estimates can be based on explosive results. Schmidt et al (1986) have presented a complete set of estimates for nuclear and conventional explosives in a variety of geologies and burial depths. It has been determined by Holsapple (1980) that explosive sources buried one to two source radii give the same crater size as an impact event with the same energy and specific energy. Using these data, estimates for impact crater size can be determined. The estimates here are a composite of those two sources. Since the estimates are unknown to within a factor of perhaps two, there is no point in retaining the ratio of the mass densities,

[9] Note that the definition of $\pi_2$ is different there by a factor of 3.22, see Footnote 3.

and it will be dropped. It could be reintroduced to give estimates of the effect of variations in impactor mass density.

Values for a range of representative geological materials are given in Table 1. Note that the estimates for the strength regime of rocks is based on relatively large craters. It thus requires sufficiently large impacts so that the effective strengths are those of the material on 10 to 100 meter scales, not cm scales. Small laboratory experiments will give much smaller craters than these estimates in such cases.[10] Figures 4 to 7 are plots for these representative materials.



## 4.2 *Ejecta*

The methods described above have been applied to the scaling of ejection dynamics and final ejecta blanket profiles by Housen et al (1983). Again, there are important distinctions depending on whether material strength or gravitational forces are the dominant mechanism determining crater size. Laboratory experiments are usually in the strength regime. Of course, once material is ejected from the crater, it is always gravitational forces that determine its ballistic path.

For brevity, only a few of the more important results of ejecta scaling are summarized here; the reader is referred to Housen et al (1983) for the complete analysis (see specifically Table 1 of that reference). Since all scaling aspects are determined by the point-source approximation, they are all given in terms of the single scaling exponent $\mu$, or equally, in terms of the exponent $\alpha$ defined in (17). Those interdependencies have often been violated in strictly empirical approaches to scaling.

Housen et al (1983) give results for the dynamics of the ejecta plume position, velocity, mass, and angle; as well as for the final blanket thickness versus range. In the gravity regime, the crater dimensions and the ejecta are both determined by the coupling parameter and by gravity. When the crater radius $R$ is used to nondimensionalize the ejecta phenomena, the dependence on the coupling parameter cancels out. The results in the gravity regime are listed in Table 2. These results show that in the gravity regime all ejecta blankets are geometrically similar to the crater size. This is not true in the strength regime, where the blanket moves relatively closer in as the crater sizes grow (see Housen et al 1983).

## 4.3 *Crater Depth and Radius*

4.3.1 SIMPLE CRATERS It is the crater radius that is most easily determined from remote observation. Consider first the so-called simple craters

[10] Very small craters in competent rocks and other brittle targets are dominated by surface spall effects rather than the excavation mechanisms of the large craters. The photo in figure 2.1 of Melosh (1989) gives a good example for a very small 30 $\mu$m crater in glass.

**Table 1** Cratering volume estimates for a variety of geological materials

| Material | Scaling exponent $\alpha$ | Scaling exponent $\mu$ | $K_1$ | $\bar{Y}$ mpa | Strength regime[a] | Gravity regime[a] | Transition impactor diameter[b] |
|---|---|---|---|---|---|---|---|
| *Sand* | *0.51* | *0.41* | *0.24* | *0* | – | $V = 0.14\ m^{0.83}\ G^{-0.51}\ U^{1.02}$ | *near 0* |
| *Dry soil* | *0.51* | *0.41* | *0.24* | *0.18* | $V = 0.04\ m\ U^{1.23}$ | $V = 0.14\ m^{0.83}\ G^{-0.51}\ U^{1.02}$ | *0.2 meters* |
| *Wet soil* | *0.65* | *0.55* | *0.20* | *1.14* | $V=0.05m\ U^{1.65}$ | $V = 0.60\ m^{0.783}\ G^{-0.65}\ U^{1.3}$ | *1.2 meters* |
| *Water* | *0.648* | *0.55* | *2.30* | *0* | – | $V = 13.0\ m^{0.783}\ G^{-0.65}\ U^{1.3}$ | *near 0* |
| *Soft rock* | *0.65* | *0.55* | *0.20* | *7.6* | $V=0.009\ m\ U^{1.65}$ | $V = 0.48\ m^{0.783}\ G^{-0.65}\ U^{1.3}$ | *11 meters* |
| *Hard rock* | *0.60* | *0.55* | *0.20* | *18* | $V=0.005\ m\ U^{1.65}$ | $V = 0.48\ m^{0.783}\ G^{-0.65}\ U^{1.3}$ | *32 meters* |

[a] Uses mass in kg, velocity in km/sec, gravity in Earth $G$'s, gives volume in $m^3$.
[b] Impactor diameter at Earth's gravity and impact velocity of 10 km/sec: it is proportional to $g^{-1}U^{-\mu}$.

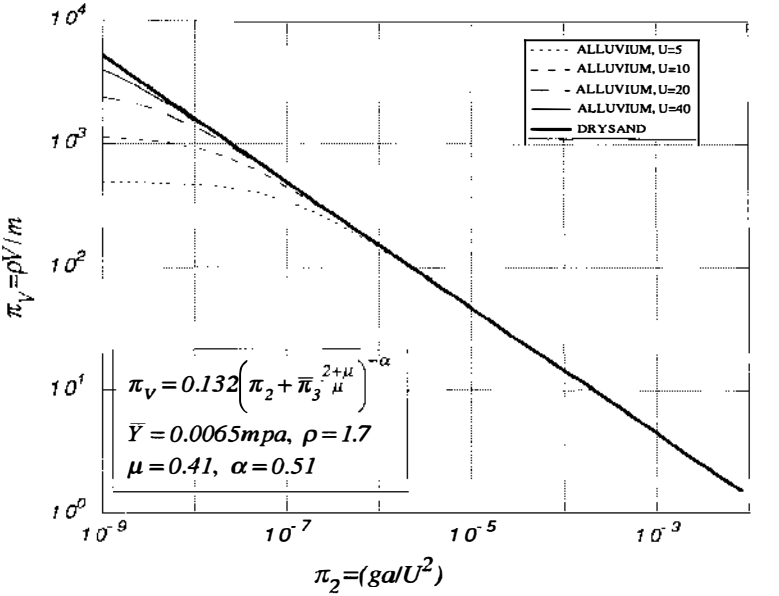


*Figure 4* Crater volume estimates for dry soils and sand showing the strength and gravity regimes. Analytical expressions are as shown. At Earth's gravity and an impact velocity of 10 km/sec, the gravity regime holds for impactor radii above about 1 m, with a corresponding crater volume of about $3 \times 10^3$ m$^3$.

which are those usual bowl-shaped craters of the laboratory and the smaller lunar and terrestrial craters. There are two radii that can be identified. Experiments usually report the radius $R_e$ measured as the radius of the crater excavation at the original ground surface. Remote observations more often use the rim radius $R_r$ measured to the top of the rim around the crater formed from the uplift and ejecta. An approach as above for either gives a law of the form

$$\pi_R = \left(\frac{\delta}{m}\right)^{1/3} R = K_1 \left[\pi_2 \left(\frac{\delta}{\rho}\right)^{1/3} + \bar{\pi}_3^{(2+\mu)/2}\right]^{-\mu/(2+\mu)}. \tag{20}$$

In the gravity regime this is

$$\left(\frac{\delta}{m}\right)^{1/3} R = K_1 (\pi_2)^{-\alpha/3} \tag{21}$$

(where the mass density ratio raised to a small power has been ignored). Schmidt & Housen (1987) give $K_1 = 0.69$ and $\alpha = 0.51$ for dry soils when

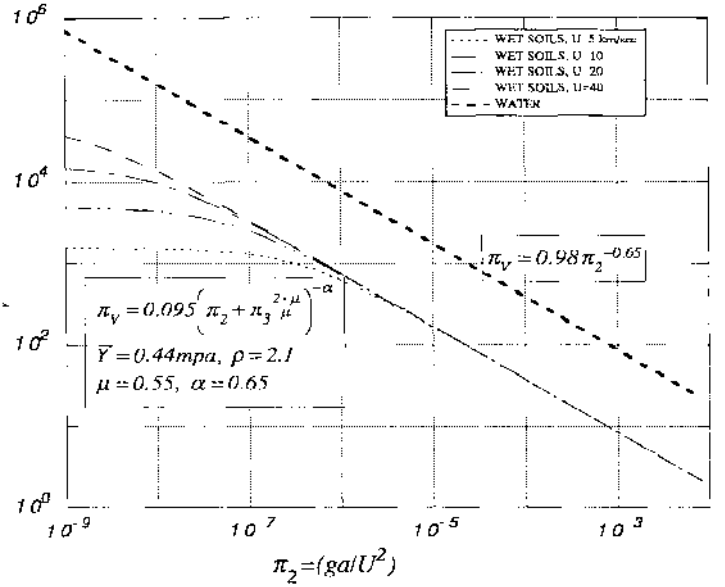


*Figure 5* Crater volume estimates for wet soils and water showing the strength (for the soils only) and gravity regimes. Analytical expressions are as shown. At Earth's gravity and an impact velocity of 10 km/sec, the gravity regime for wet soils holds for impactor radii above about 1 m, with a corresponding crater volume of about $2 \times 10^4$ m$^3$.

converted to this form for the excavation radius $R_e$. This can be expanded to

$$R_e = 7.8G^{-0.17}a^{0.83}U^{0.34} \tag{22a}$$

using the same ($m, G$, km/sec) units as in Table 1. The radius to the rim peak around the crater has the same scaling, but with a different coefficient. The measurements of the rim profiles reported by Housen et al (1983) for dry soils give the rim peak at a factor of 1.3 of the excavation radius. In either the strength or gravity regime any linear dimension will follow the same type of scaling law, so the crater shapes are similar at all sizes (but could be different in each regime). Therefore the ratio of rim radius to excavation radius is constant. Thus

$$R_r = 10.14G^{-0.17}a^{0.83}U^{0.34}. \tag{22b}$$

The reader is referred to Schmidt & Housen (1987) for other estimates of this form for wet and dry soils and for water.

Two crater depths can also be identified: that below the rim peak $d_r$,

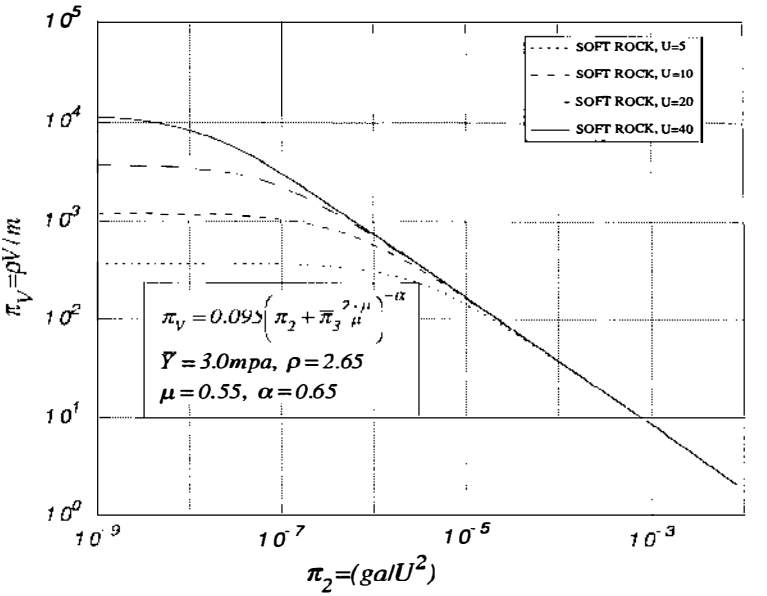


*Figure 6* Crater volume estimates for soft rocks showing the strength and gravity regimes. Analytical expressions are as shown. At Earth's gravity and an impact velocity of 10 km/sec, the gravity regime holds for impactor radii above about 10 m, with a corresponding crater volume of about $4 \times 10^6$ m$^3$.

and that excavated below the original ground surface $d_e$—the difference being the rim height $h$. Experimental craters in an alluvial soil show an aspect ratio $R_e/d_e$ just over 2 for shallow buried explosions in an alluvial soil, and a rim height $h/R_e$ of about 0.07 (Schmidt et al 1986). Pike (1977) shows a constant value of about 2.55 for $R_r/d_r$ and $h/R_r = 0.072$ for lunar craters from a diameter of 0.1 km up to a crater diameter of about 15 km. These are all approximately consistent. Thus, for the depth $d$, one can simply use (22b) divided by 2.55, and for the rim height $h$ can multiply (22b) by 0.07 to get

$$d_r = 4.0G^{-0.17}a^{0.83}U^{0.34} \tag{22c}$$

for the depth below the rim, and

$$h = 0.71G^{-0.17}a^{0.83}U^{0.34} \tag{22d}$$

for the rim height.

4.3.2 COMPLEX CRATERS For the larger craters, additional phenomena occur. In contrast to the results for the smaller craters, the observed aspect ratio is no longer constant but increases rapidly with increasing crater

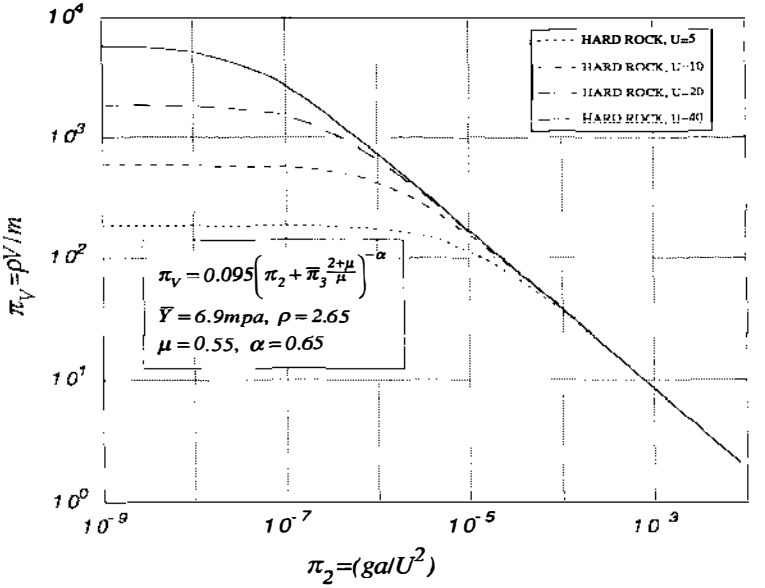


*Figure 7* Crater volume estimates for hard rocks showing the strength and gravity regimes. Analytical expressions are as shown. At Earth's gravity and an impact velocity of 10 km/sec, the gravity regime holds for impactor radii above about 20 m, with a corresponding crater volume of about $2 \times 10^7$ m$^3$.

**Table 2** Scaling of cratering ejecta[a]

| Ejecta characteristic | Gravity regime results |
|---|---|
| Plume Position $x$ versus Time t | $x/R \propto \left(t\sqrt{g/R}\right)^{2\alpha/(\alpha+3)}$ |
| Velocity $v$ versus Position $x$ | $v/\sqrt{gR} \propto (x/R)^{(\alpha-3)/2\alpha}$ |
| Velocity versus Time | $v/\sqrt{gR} \propto \left(t\sqrt{g/R}\right)^{(\alpha-3)/(\alpha+3)}$ |
| Volume Ejected at Velocity > $v$ | $V_e/R^3 \propto \left(v/\sqrt{gR}\right)^{6\alpha/(\alpha-3)}$ |
| Volume Ejected at Position < $x$ | $V_e/R^3 \propto (x/R)^3$ |
| Blanket Thickness $B$ versus Range $r$ | $B/R \propto (r/R)^{(6+\alpha)/(\alpha-3)}$ |

[a] From Housen et al 1983.

diameter. Pike (1977) shows that, for craters with a diameter greater than 20 km, the depth below the rim scales with the rim radius as $d_r \propto R_r^{0.3}$ so that $R_r/d_r \propto R_r^{0.7}$. That fact, and the obvious morphological changes for the larger craters, are affirmation of a new mechanism for large craters—generally thought to be a collapse of simple craters above a certain threshold size (15 to 20 km diameter on the Moon, 3 km on the Earth) due to gravitational forces, leading ultimately to the *complex* craters having central peaks, terraced walls, and circular rings. That the transition occurs on several different bodies (the Earth, Moon, Mercury, and Mars; see Pike 1988) at a value inversely proportional to the surface gravity argues strongly for this gravity-driven mechanism (assuming roughly equal crustal strengths).

Thus, when a simple crater is sufficiently large, there apparently occurs a final "gravity-modification" stage of formation. Any shape described by the scaling laws given above will collapse and perhaps, if large enough, oscillate to form the large basins observed, with resulting topologies of slumped walls, terraces, and central peaks. The final resting state of the crater in those cases then will have a much smaller depth and somewhat greater radius than that predicted from (22). However, since this slumping is to first order volume conserving, the volume scaling will not show this effect, and the results above may be applied. (If anything, because of bulking, the crater volume may decrease during these processes, making the predictions given an upper bound. However, over long time periods any low density material may be expected to consolidate back to its initial density by natural processes.)

Thus, for the scaling of the radius and depth the final resting configuration can no longer be simply assumed to depend on the gravity field, since the slumping and final configuration must be determined by some material strength measure. There reappears a dependence on both the gravity (determining the transient crater) and on some strength (determining when the crater is "frozen" into its final configuration). The additional dependence on a material strength will give another transitional regime and the appropriate scaling law for the crater radius may appear as shown schematically in Figure 8.

A simple scaling approach to this problem will be outlined. If the slumping and rebound phenomena are effectively uncoupled from the transient crater stages of the formation, then either of the above Equations (22) for the gravity regime can be used directly for a maximum transient[11]

[11] In some cases, it is also important to distinguish between a maximum transient crater and a final resulting simple crater shape. The radii of those two are nearly equal, but the depth of the maximum transient crater is typically a factor of two larger than the final simple crater due to rebound mechanisms. See the measurements by Schmidt & Housen (1987).

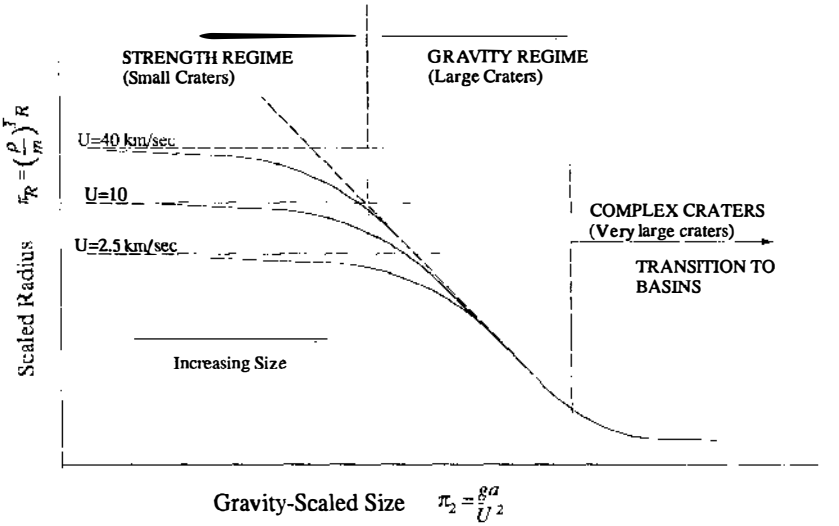


*Figure 8* Schematic cratering curves for crater radius, showing an additional "complex crater" regime for very large craters. At Earth's gravity, the strength regime holds for submeter sized craters, the gravity regime for meter to km sizes, and the transition to complex craters begins at diameters of a few kilometers.

crater rim radius $R_t$. The subsequent crater modification stage does not depend at all on the impactor conditions but only on this transient crater size, on gravity, on the mass density of the material, and on some material strength, so that the final rim radius is given by

$$R = f(R_t, \rho, g, Y) \tag{23}$$

which has the dimensionless form

$$\frac{R}{R_t} = f\left(\frac{\rho g R_t}{Y}\right). \tag{24}$$

Thus, there is a single unknown function to be determined. (Earlier approaches have often assumed a constant function, e.g. $f = 1.3$.) This relation will hold only when the crater radius is greater than some transitional crater radius denoted by $R_*$. At that transition $R_t = R_*$ and also $R = R_*$ so that the function must be unity when $R_t = R_*$.

This means

$$R_* \propto \frac{Y}{\rho g} \tag{25}$$

so that the transition radius is proportional to some strength measure and inversely proportional to the gravity. Substituting this back into (25) gives a useful form which eliminates the unknown strength in terms of the observable transition radius:

$$\frac{R}{R_t} = f\left(\frac{R}{R_*}\right). \tag{26}$$

It is tempting to introduce the usual power laws for this function; but, in contrast to the developments above, here there is no obvious theoretical reason for such. It is clear though that the function must be unity for craters below the transition size $R_*$, and an increasing function above that threshold.

In the past, there have been several authors who considered this problem, most recently Croft (1985). Croft does succumb to the temptation: He assumes as his working hypothesis that the final radius is a power law in the initial energy, with an additional dependence on the velocity. He obtains a relation like

$$\frac{R}{R_t} = \left(\frac{R}{R_*}\right)^{\beta} \tag{27}$$

as a special form for (26). [A more direct approach would be to simply assume that the final radius depends only on the transient shape as in (24), and assume a power law there. Then one again obtains relation (27).] Croft (1985) examined four different criteria based on extensive lunar observations and chose the exponent $\beta$ as 0.15. One of those criteria was an assumption of the constancy of the volume in a slumping process, which uses various earlier empirical forms for crater geometry features. Melosh (1989) also presents an argument based on constant volume, together with the simple power-law analytical forms for the ejecta blanket thickness that hold for energy scaling in the far field.

A new analysis (Holsapple, unpublished) is also based on the assumption of constant volume in a slumping mechanism, but with several improvements over the previous analyses. The actual crater shapes and the rim profiles as measured by Schmidt et al (1986) and Schmidt & Housen (1987) were used, rather than a simple analytical power-law model appropriate for the far field only. The crater scaling given here was used for the shape and volume of the simple craters. The morphometric data of Pike (1977) for actual lunar craters gives a basis for determining their volume as a function of the final radius $R$. Then the extent of the crater slumping can be determined, and a particular function as in (26) determined. The final results of this analysis are as shown in Figure 9.

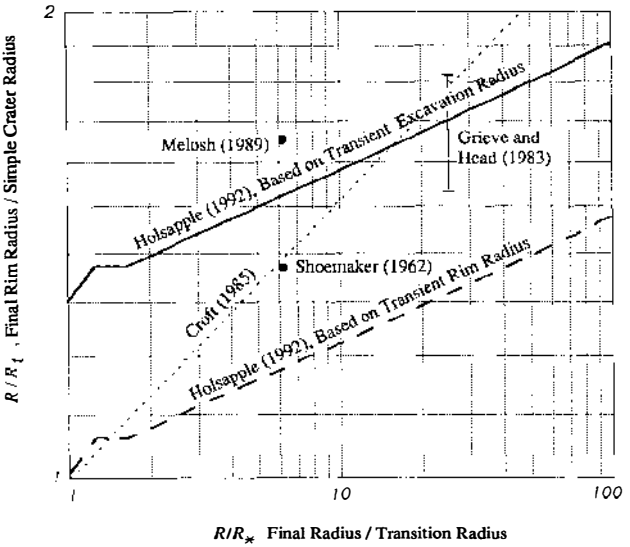


*Figure 9* Radius enhancement due to gravity-modification slumping mechanisms based on a constant volume model of the author and observed simple crater profiles.

There are two curves shown, one the ratio of the final rim radius $R$ to the transient *rim* radius $R_r$ and one the ratio of the final rim radius to the transient *excavation* radius $R_e$. Previous studies have not distinguished between these, and there is a factor of 1.3 difference. Either curve is essentially a power law over most of the domain of interest. These results seem to be as consistent with the large variety of observed features given by Croft (1985) as is his power-law estimate. The Shoemaker (1962) estimate for Copernicus seems to be for the ratio of rim radii, so the present result is definitely below it. The Melosh (1989) estimate for Copernicus is based on a model that has no difference in the two radii. The Grieve & Head (1983) estimate for the 100 km diameter terrestrial crater Manicouagan is most applicable to the ratio using the transient excavation radius, and the present result agrees well.

For analytical calculations, the fit to the functions shown are

$$\frac{R}{R_r} = 1.02\left(\frac{R}{R_*}\right)^{0.079}, \quad \frac{R}{R_e} = 1.32\left(\frac{R}{R_*}\right)^{0.079} \tag{28}$$

for the ratios of the final to either of the transient excavation or rim radius.

Since the ratio of the radius $R$ to the transition radius $R_*$ can be directly observed, this result (28) can be used to determine the original transient

radius in terms of the observed final radius $R$. Then (22) applied to $R_t$ gives the impactor conditions.

For lunar craters the results are as shown in Figure 10. The transition is taken at a crater radius of 8.5 km, the value where the volume given by the scaling of simple craters here equals that determined by the Pike (1977) data. (This plot does not show the strength-dominated craters that would occur for smaller diameters.)

The depth scaling for complex lunar craters was obtained by using the rule

$$\frac{d}{R_*} = 0.313\left(\frac{R}{R_*}\right)^{0.301} \tag{29}$$

for complex craters—a dimensionless form equivalent for lunar craters with that given by Pike (1977). Note that the final depth is much reduced from the transient; at 100 times the transition size, the depth is reduced by a factor approaching 20 of the predicted simple crater depth (a factor of

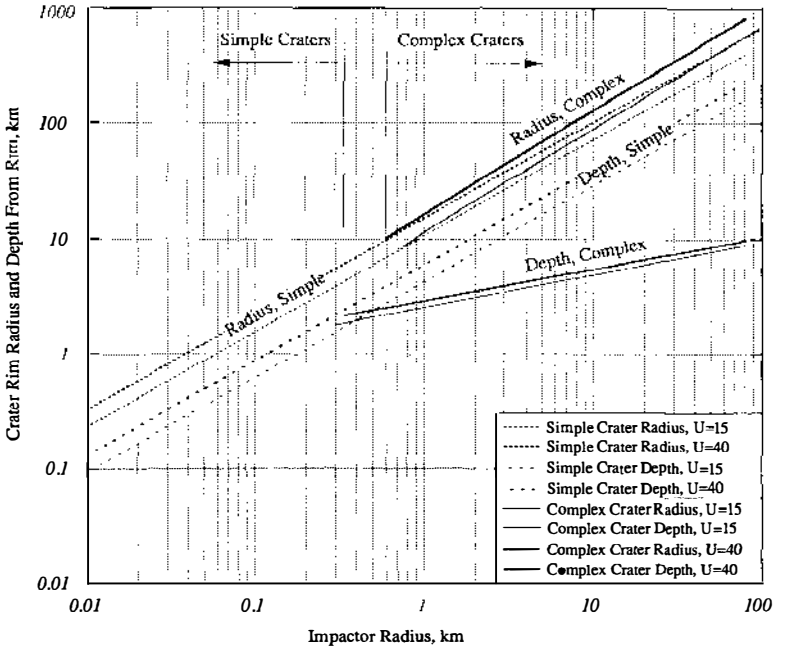


*Figure 10* Crater radius and depth for lunar craters showing both the transitory simple crater and the final complex crater sizes.

40 less than the maximum transient crater). The radius is enlarged by a factor of almost 1.5 from the excavation radius, and a factor of about 1.9 from the simple rim radius.

The scaling of these last two sections implies that the impact on the Moon of a 25 km radius impactor traveling at 25 km/sec would first excavate a simple crater with a depth below the rim of about 72 km (using 22c), an excavation radius of 141 km (using 22a), a transient rim radius of 184 km (using 22b), with a previous transient depth of about 150 km. Then, during the gravity modification stage (using Equation 28b), this structure reforms to a depth of "only" 7.3 km and to a radius of 244 km. While an initial excavation to such great depths may seem surprising, code calculations of large impact structures produce similar results (see Roddy et al 1987).



## 4.4 *The Dynamics of Crater Formation*

In addition to the final crater, the methods here can also be applied to the actual dynamics of the shock propagation and the crater growth history. The key is the assumption that a single combined coupling parameter measure is appropriate, and that it must determine all aspects of the event. Measurements of observations of any one suffice to give that exponent, and the scaling of any other aspect can be predicted. Dynamic facets include the time of formation (Schmidt & Housen 1987), the shock pressure decay, the transient crater growth history (Holsapple 1984, Holsapple & Schmidt 1987), and others.

Tables 3 and 4 give a variety of results for the dynamics of the crater history. Shown are a general case and six specific special regions that can be identified. (In some cases, the regimes overlap.) Two examples of the use of this table, and a discussion of the various regimes will be given.

4.4.1 SHOCK PRESSURE PROPAGATION AND DECAY Consider the peak pressure $P$ at the shock wave formed from the impact event. Figure 11 shows a schematic of its decay with range or with time. That pressure can depend on the variables shown in the second column of Table 3, namely $\rho$, $U$, $a$, $c$, $Y$, $r$, $t$, where $c$ is a sound speed measure of the material. For the initial value at the instant of contact ($r = 0$, $t = 0$), the pressure is typically substantially above any strength measure, so the strength $Y$ can be ignored; and usually the impact velocity is substantially above the wave speed $c$, so it too can be dropped. [If the impact velocity is not large compared to the sound speed, then the sound speed $c$ must be retained, and the dimensional analysis yields $P/(\rho U^2) = f(c/U)$. The exact value can be obtained by the usual impedance matching approach.] Furthermore,

**Table 3** Scales for impact processes for initial values and near-source regions

| | General | Initial | Near source |
|---|---|---|---|
| Defined by: | | $r = 0,\ t = 0$ | $r \approx a$ |
| Variables: | $\rho, U, a, c, Y, r, t$ | $\rho, U, a$ | $\rho, U, a, r$ (or $t$) |
| Pressure | $\rho U^2, \rho c^2, Y$ | $\rho U^2$ | $\rho U^2 f(r/a)$ |
| Velocity | $U, c, \sqrt{Y/\rho}$ | $U$ | $U\ f(r/a)$ |
| Time, Durations | $a/U, t$ | $a/U$ | $a/U\ f(r/a)$ |
| Position, Length | $a, r$ | $a$ | $a\ f(r/a)$ |

**Table 4** Scaling of cratering events away from source region, as governed by the point-source approximation

| | Strong shock | Intermediate | Special intermediate | Weak shock |
|---|---|---|---|---|
| Defined by: | $P >> \rho c^2,\ r \approx 2-3$ | $P \approx \rho c^2$ | Shock speed $\approx c$ | $P \approx Y$ or $\rho g h$ |
| Variables: | $\rho, aU^\mu, r$ (or $t$) | $\rho, aU^\mu, c, r$ (or $t$) | $\rho c, aU^\mu, r$ (or $t$) | $\rho, aU^\mu, c, Y, r$ (or $t$) |
| Pressure | $\rho U^2 (a/r)^{2/\mu}$ | $\rho U^2 (a/r)^{2/\mu} f\left((c/U)(a/r)^{-1/\mu}\right)$ | $\rho c U (a/r)^{1/\mu}$ | $f$ also has $(Y/\rho c^2)$ |
| Velocity | $U(a/r)^{1/\mu}$ | $U(a/r)^{1/\mu} f\left((c/U)(a/r)^{-1/\mu}\right)$ | $U(a/r)^{1/\mu}$ | $f$ also has $(Y/\rho c^2)$ |
| Time, Durations | $(a/U)(r/a)^{(1+\mu)/\mu}$ | $(a/U)(r/a)^{(1+\mu)/\mu} f\left((c/U)(a/r)^{-1/\mu}\right)$ | $(a/U)(r/a)^{(1+\mu)/\mu}$ | $f$ also has $(Y/\rho c^2)$ |
| Position, Length | $a(Ut/a)^{\mu/(1+\mu)}$ | $a(Ut/a)^{\mu/(1+\mu)} f\left((c/U)(Ut/a)^{1/(1+\mu)}\right)$ | $a(Ut/a)^{\mu/(1+\mu)}$ | $f$ also has $(Y/\rho c^2)$ |

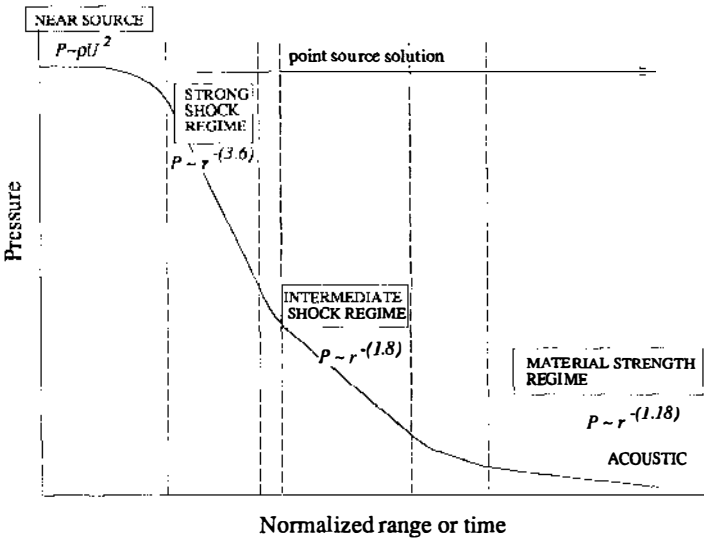


*Figure 11* The regimes of the evolution of the peak pressure at the shock for the outgoing shock wave in an impact problem.

the finite curvature of the impactor is not yet a factor, so that the radius $a$ can also be dropped. That leaves only the two variables $\rho$ and $U$. A dimensional analysis then gives the result shown in the third column of Table 3: $P \propto \rho U^2$. This is indeed the result obtained by a simple one-dimensional "impedance-matching" solution for an impact. (The introduction of a specific Hugoniot result such as a linear shock-particle velocity relation will give the constant of proportionality of this relation again by using the impedance matching approach of shock mechanics.)

This initial shock will then move into the interior of the body and form a nearly hemispherical shock which decays in magnitude as it propagates. The peak pressure at the shock is then a function of position $r$ (or of time $t$). When $r$ is on the order of the impactor radius $a$, that radius must be retained in a dimensional analysis which gives (assuming the case when $U \gg c$) $P = \rho U^2 f(r/a)$, as in the fourth column of Table 3. Similar results are obtained for the particle velocity at thc shock, for the time duration of the pulse, and its position.

After the shock moves a few impactor radii away from the impact point, the problem transitions to one governed by a point source, as measured by the coupling parameter. In general, the problem can still show three distinct regimes, depending on the magnitude of the pressure. These three

possible regimes are called the "strong-shock," the "intermediate," and the "weak shock" regimes. There is often a fourth regime which is labeled as the "special intermediate" in Table 4.

The strong shock regime is defined as one for which the particle velocities are still much larger than the sound speed $c$. Equally, the pressure $P \gg \rho c^2$. However, there cannot be a separate dependence on the impactor velocity $U$ and its radius $a$ in this regime, since the point-source approximation governs.[12] The second column of Table 4 then shows the results of a dimensional analysis, $P = \rho U^2 (a/r)^{2/\mu}$, giving a power-law decay of shock front pressure with distance. The particle velocity at the shock decays with distance to the power of $1/\mu$.

As that decay progresses, the pressure will ultimately become comparable to the pressure scale $\rho c^2$. Then the sound speed $c$ again reenters the analysis, giving the less specific results shown in the "intermediate regime." However, usually the power-law result for the velocity holds to much greater ranges than that for the pressure, even when the shock velocity is comparable to the sound speed. In that case, the pressure at a shock is linear in the particle velocity, as is apparent from the jump conditions. Thus, since the velocity decays to the power of $1/\mu$, so does the pressure (see the "special intermediate" case in Table 4).

Finally, in the very far field, the pressure will decay to a level comparable to either a material strength $Y$, or perhaps to some initial pressure $P_0$, as in an air-blast analysis. Then the peak pressure also depends on this additional stress measure, as shown in the final column of Table 4.

It is important for the reader to remember that the scaling powers of these laws use exactly the same exponent $\mu$ as the size scaling. Thus, for nonporous material such as rock or water, the appropriate value is about $\mu = 0.55$. Recent papers by O'Keefe & Ahrens (1992a,b) have verified that fact by a suite of code calculations of the cratering dynamics for generic nonporous materials. (Once one accepts the governance of the point-source solution, then a single calculation at any suitable size and velocity suffices to define all of the point-source solution regime.) The reader can refer to these papers for specific numerical forms for those materials for the scaling laws given here.

4.4.2 DYNAMIC CRATER GROWTH The scaling of any length scale is shown in the last row of the Table 3. It can be applied to the transient crater growth history (Holsapple 1984, Holsapple & Schmidt 1987). During the

[12] The literature is full of errors regarding this point. Some assume that the time scale and rise time of the far-field pulse is $a/U$, which in fact can only hold very near the impactor, as shown in the appropriate row of Table 2. Away from the impact point, every dependence on the impactor conditions must be in a combined form $aU^{\mu}$.

initial regime the projectile buries itself in the planet at a constant velocity equal to the particle velocity behind the shock as determined by the jump conditions. Therefore, the projectile/planet interface surface moves at a constant velocity in this "penetration" regime. After a distance of just over one projectile radius the transition to the point-source solution is apparent, and the interface moves according to the power of $\mu/(1+\mu)$ in time, as in the first column of Table 4. That slope governs until just before the crater begins to slow its growth at the maximum transient depth. After maximum depth is achieved, there is a rebound of up to a factor of two to the final observed simple crater depth. Figure 12 (reproduced from Holsapple & Schmidt 1987) clearly demonstrates these regimes and, further, shows the commonalty of the dynamic growth in a wide variety of different materials when scaled according to these laws, and provides numerical values. O'Keefe & Ahrens (1991) clearly identify these same results for a single material in a suite of code calculations at various impactor sizes and



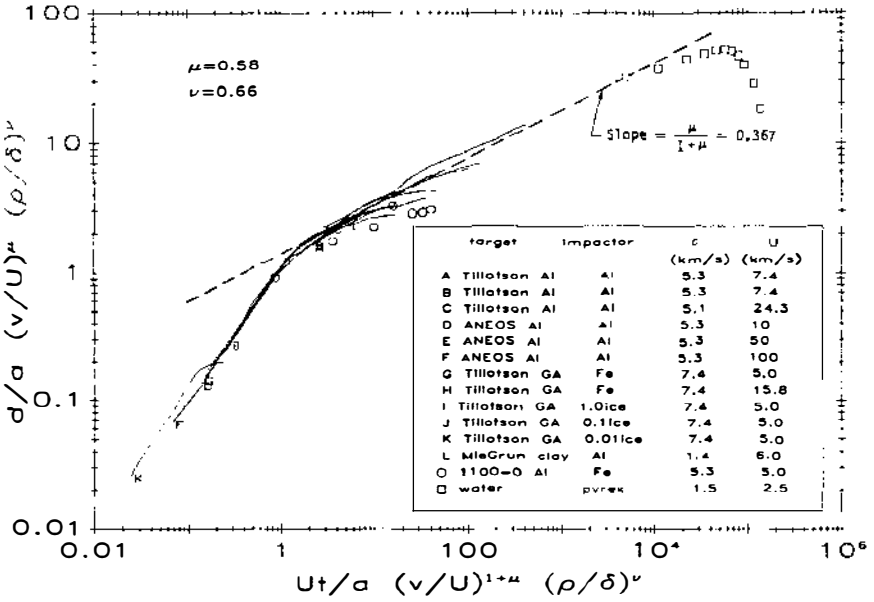


*Figure 12* The growth of transient crater depth with time from experiments and calculations for a variety of conditions. In this scaled form all follow a common path, with an early time "penetration" regime and an intermediate time "point-source" regime. The growth is ultimately arrested by either a material strength or the gravity, depending on the conditions.

gravities. O'Keefe & Ahrens (1992b) give many numerical formulas for these specific forms for that material.[13]

## 5. CATASTROPHIC IMPACTS

The catastrophic disruption of asteroids and other solar system bodies is another inevitable consequence of energetic impacts, and another important application of impact scaling. Theories of collisional fragmentation are at present more speculative than for cratering. Most of our knowledge of such events is based on experimental results. Unfortunately, due again to practical constraints, the experiments are conducted at size and velocity scales that are vastly different from those appropriate to collisions involving asteroids or satellites. Therefore the results must be extrapolated using scaling rules.

Scaling rules that guide the extrapolation of small-scale results can be based on the same concepts as for cratering. The most common scaling method in the previous literature assumes that collisional outcomes (e.g. normalized fragment size and velocity distributions) are determined by the energy of the event divided by the mass of the target body, i.e. by the ratio $Q = E/M$. A specific value $Q_*$ determines the threshold for catastrophic disruption, which is defined as when the largest remaining fragment is 1/2 the size of the original body. This threshold specific energy for target fragmentation is typically assumed to be independent of target size and impact velocity. That approach mirrors the older energy-scaling assumptions for cratering. In addition, it is implicitly based on an assumption that the asteroid strength is independent of size and rate. On the basis of a variety of experimental and theoretical evidence, it now appears that neither of these conditions should hold, thereby casting serious doubt on the validity of using $Q$ as the sole parameter in scaling.

For cratering, the predominant strength measure is the yield function that limits shear stresses, as for example, a Mohr-Coulomb law. In contrast, the disruption of entire bodies is governed more by a tensile fracture strength measure. For geological materials such as rock and for other brittle materials, fracture strength is typically highly strain-rate dependent. In addition, for large bodies gravitational self-compression

[13] While they also give results for final crater size, it is difficult to predict final outcomes using numerical approaches. This author believes that the code approaches are better believed for study of the earlier regimes of impact processes, and for relative comparisons of different conditions; not for absolute measures of the final outcome. In particular, codes have extreme difficulty in calculating impact processes for any material with porosity.

deters fragmentation. Both factors must be accounted for in developing scaling theories for catastrophic disruptions.

Holsapple & Housen (1986) and Housen & Holsapple (1990) have considered this problem in detail. The interested reader is referred to these references for the complete analysis and discussion. The situation is similar to the scaling above for cratering. As long as the impactor is relatively small compared to the body being impacted, then the coupling parameter measure can be adopted, greatly simplifying the dependence on the impactor conditions. (While this becomes more of a problem than for cratering, catastrophic disruptions typically occur with the impactor to impacted body diameters in the ratio of about 1:10.)

Again there are two obvious regimes. For smaller bodies gravitational attractions between the parts of the body can be ignored. (Typically these are for asteroids small enough to be nonspherical.) Then one can assume a single measure for the strength of the body. However, as mentioned already, that measure should now be rate-dependent.

The fracture of brittle materials is a consequence of the growth and coalescence of an initial distribution of various sizes of small flaws and cracks. At any material point, all cracks with a length greater than some critical length—which depends on the instantaneous stress level—will be activated and growing. Fracture occurs whenever any crack lengths are able to grow to their inter-crack spacing, and that spacing will determine the dominant fragment sizes.

In a simple constant strain-rate test, the resulting fracture strength based on this model is in accord with the common strain-rate dependent model

$$\sigma_{cr} = S\dot{\varepsilon}^{1/n}, \tag{30}$$

where the exponent $n$ is given by the original crack size distribution, and the coefficient $S$ is a material constant. (The model also predicts fracture strength for more general stress histories, when the strength is not simply proportional to a power of the instantaneous strain rate.) Holsapple & Housen (1986) then used this material measure $S$ for the resisting measure for disruption, together with the coupling parameter as the measure of the input, to determine a variety of scaling results. A further dependence on gravitational forces was allowed, and it dominates for the larger bodies.

One of the more fundamental results is shown as Figure 13, for the threshold specific energy dependence on target body size, as presented in Housen et al (1991). [This figure supersedes the earlier estimates given in Housen & Holsapple (1990); it is based on the theory and recent experiments.] In contrast to the energy-scaling, constant strength approach, the inclusion of a rate dependence for the fracture strength makes the threshold specific energy $Q$ decrease for increasing target size in the strength regime,

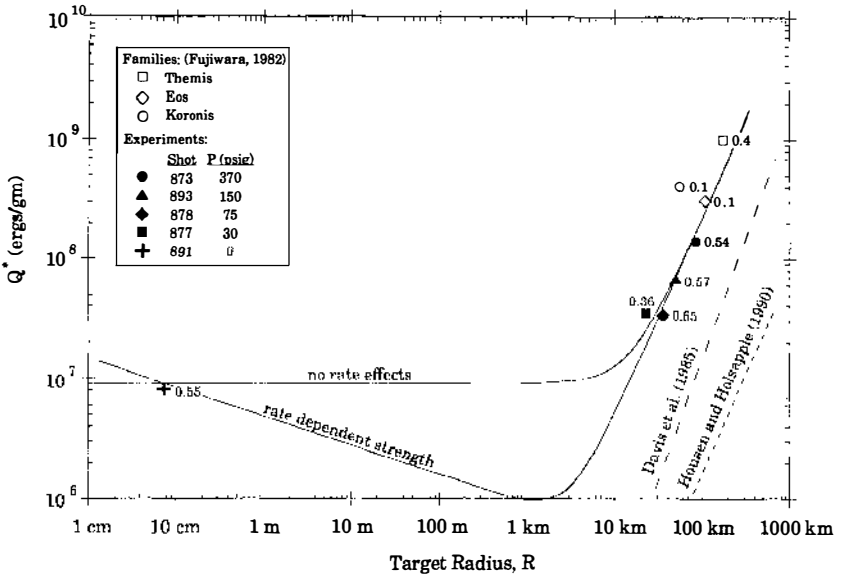


*Figure 13* Estimates of the specific energy required to catastrophically break an asteroid. (From Housen et al 1991.)

due to the fact that the larger events have a correspondingly slower stress pulse and thus a weaker governing strength compared to small laboratory events. Then, for bodies more than about 2 km in diameter, the gravitational forces become the dominant factor, and the threshold energy required again increases.

## 6. CONCLUDING REMARKS

Much has been learned about scaling over the past decade. Much of that progress is based on the recognition of the point-source approximation as the appropriate simplifying assumption that leads to the power-law results empirically observed; and, as a consequence, the earlier energy-scaling assumptions are replaced with the coupling parameter measure approach. However, there remains much to be learned. The theories presented here are only of first order—a "child's garden of scaling." The specific scaling laws are generally based on two ingredients: a choice of the measure of the "input" (i.e. the coupling parameter measure of the impactor), and a choice of a single measure of a "resistance" (c.g. a single strength or gravity). Many complicating factors exist which are not presently quantified, and will lead to future research.

More study is certainly needed about:

1. Scaling when the crater becomes so small compared to the impactor that the point-source assumption is not appropriate;
2. Atmospheric effects such as might be important on Venus and the Earth;
3. Facets of cratering such as the melt and vapor produced in the near field that are not governed by far-field scaling;
4. Layered and inhomogeneous targets, which must affect the immense transient depths of large craters, or for impacts into the ocean floor;
5. Very small craters where surface tension and viscosity of the material play roles;
6. Impacts on the icy satellites;
7. Subsequent creep mechanisms of materials including ice, and how they change the observed craters;
8. Highly oblique impacts;
9. Very low speed interactions of reaccumulation processes and planetary growth;
10. Dispersed impactors, such as asteroids or comets fractured during atmospheric penetration;
11. The gravity modification stage for complex craters and for the very large basins and ring structures;
12. Impacts of comparable sized bodies;
13. Details of escape mechanisms for near surface material.

## ACKNOWLEDGMENTS

The research reported here has been supported by funding from the NASA Planetary Geology and Geophysics Program under grant NAGW-328. I thank my colleagues and critics K. R. Housen and R. M. Schmidt, who were co-investigators and coauthors for many of the results reported.

*Literature Cited*

Barenblatt, G. I. 1979. *Similarity, Self-similarity, and Intermediate Asymptotics.* New York: Consultants Bureau

Croft, S. K. 1985. The scaling of complex craters. *Proc. Lunar Sci. Conf. 15th. J. Geophys Res.* 90: C828–42 (Suppl.)

Dienes, J. K., Walsh, J. M. 1970. Theory of impact: some general principles and the method of Eulerian codes. In *High-Velocity Impact Phenomena*, ed. R. Kinslow. New York: Academic

Fujiwara, A. 1982. Complete fragmentation of the parent bodies of the Themis, Eos, and Koronis families. *Icarus* 52: 434–43

Gault, D. E. 1978. Experimental impact "craters" formed in water: gravity scaling realized. *Eos Trans. Am. Geophys. Union* 59: 1121 (Abstr.)

Gault, D. E., Wedekind, J. A. 1977. Experimental hypervelocity impact into quartz sand, II, Effects of gravitational acceleration. See Roddy et al 1977, pp. 1231–44

Grieve, R. A. F., Head, J. W. 1983. The Manicouagan impact structure: an analysis of its original dimensions and form.

*Proc. Lunar Planet. Sci. Conf.* 13*th*, *J. Geophys. Res.* 88: A807–18

Holsapple, K. A. 1980. The equivalent depth of burst for impact cratering. *J. Geochem. Soc. Meteoritical Soc., Suppl.* 14, pp. 2379–2401

Holsapple, K. A. 1981. Coupling parameters in cratering. *Eos Trans. Am. Geophys. Union* 62(45): 944 (Abstr.)

Holsapple, K. A. 1982. A Comparison of scaling laws for planetary impact cratering: experiments, calculations and theory. *Lunar Planet. Sci. XIII*, p. 331

Holsapple, K. A. 1983. On the existence and implications of coupling parameters in cratering mechanics. *Lunar Planet. Sci. XIV*, pp. 319–20

Holsapple, K. A. 1984. On crater dynamics: comparisons of results for different target and impactor conditions. *Lunar Planet. Sci. XV*, pp. 367–68

Holsapple, K. A. 1987. The scaling of impact phenomenon. *Int. J. Impact Eng.* 5: 343–55

Holsapple, K. A., Housen, K. R. 1986. Scaling laws for the catastrophic collisions of asteroids. *Mem. Soc. Astron. Ital.* 57(1): 65–85

Holsapple, K. A., Schmidt, R. M. 1979. A material strength model for apparent crater volume. *J. Geochem. Soc. Meteoritical Soc., Suppl.* 13, pp. 2757–77

Holsapple, K. A., Schmidt, R. M. 1982. On the scaling of crater dimensions 2. Impact processes. *J. Geophy. Res.* 87(B3): 1849–70

Holsapple, K. A., Schmidt, R. M. 1987. Point-source solutions and coupling parameters in cratering mechanics. *J. Geophys. Res.* 92(B7): 6350–76

Housen, K. R., Holsapple, K. A. 1990. On the fragmentation of asteroids and planetary satellites. *Icarus* 84: 226–53

Housen, K. R., Schmidt, R. M., Holsapple, K. A. 1991. Laboratory simulations of large scale fragmentation events. *Icarus* 94: 180–90

Housen, K. R., Schmidt, R. M., Holsapple, K. A. 1983. Crater ejection scaling laws: fundamental forms based on dimensional analysis. *J. Geophys. Res.* 88: (B3): 2485–99

Lampson, C. W. 1946. Explosions in earth. In *Effects of Impact and Explosion V.*1, Chap. 3, p. 110. Washington, DC: Off. Sci. Res. Dev.

Melosh, H. J. 1989. *Impact Cratering, A Geological Process.* New York: Oxford Univ. Press

Oberbeck, V. R. 1977. Application of high explosion cratering data to planetary problems. See Roddy et al 1977, pp. 45–66

O'Keefe, J. D., Ahrens, T. J. 1991. Tsunamis from giant impacts. *Lunar Planet. Sci. XXII*, pp. 997–98

O'Keefe, J. D., Ahrens, T. J. 1992a. Melting and shock weakening effects on impact crater morphology. *Lunar Planet. Sci. XXIII*, pp. 1017–18

O'Keefe, J. D., Ahrens, T. J. 1992b. Planetary cratering mechanics. Submitted

Pike, R. J. 1977. Size-dependence in the shape of fresh impact craters on the moon. See Roddy et al 1977, pp. 489–509

Pike, R. J. 1988. Geomorphology of impact craters on Mercury. In *Mercury*, ed. F. Vilas, C. R. Chapman, M. Shapley-Matthews, pp. 165–273. Tucson: Univ. Ariz. Press

Rae, W. J. 1970. Analytical studies of impact-generated shock propagation: survey and new results. In *High-Velocity Impact Phenomena*, ed. R. Kinslow. New York: Academic

Roddy, D. J., Schuster, S. H., Rosenblatt, M., Grant, L. B., Hassig, P. J., Kreyenhagen, K. N. 1987. Computer simulations of large asteroid impacts into oceanic and continental sites—preliminary results on atmospheric, cratering and ejecta dynamics. *Int. J. Impact Eng.* 5: 525–41

Roddy, D. J., Pepin, R. O., Merrill, R. B., eds. 1977. *Impact and Explosive Cratering*, New York: Pergamon

Schmidt, R. M. 1977. A centrifuge cratering experiment: development of a gravity-scaled yield parameter. See Roddy et al 1977, p. 1261–78

Schmidt, R. M. 1980. Meteor Crater: energy of formation—implications of centrifuge scaling. *Proc. Lunar Sci. Conf.* 11*th*, pp. 2099–2128

Schmidt, R. M., Holsapple, K. A. 1978a. A gravity-scaled energy parameter relating impact and explosive crater size. *Eos Trans. Am. Geophys. Union* 59(12): 1121 (Abstr.)

Schmidt, R. M., Holsapple, K. A. 1978b. Centrifuge cratering experiments in dry granular soils. *DNA Rep.* 4568*F*. Washington, DC: Defense Nucl. Agency

Schmidt, R. M., Holsapple, K. A. 1980. Theory and experiments on centrifuge cratering. *J. Geophys. Res.* 85: 235–52

Schmidt, R. M., Holsapple, K. A. 1982. Estimates of crater size for large-body impact: gravity-scaling results. *Geol. Soc. Am. Spec. Pap. No.* 190

Schmidt, R. M., Holsapple, K. A., Housen, K. R. 1986. Gravity effects in cratering. DNA Rep. DNA-TR-86-182. Washington, DC: Defense Nucl. Agency

Schmidt, R. M., Housen, K. R. 1987. Some recent advances in the scaling of impact

and explosion cratering. *Int. J. Impact Eng.* 5: 543–60
Sedov, L. I. 1946. *Appl. Math. Mech. Leningrad* 10(2): 241
Shoemaker, E. M. 1962. Interpretation of lunar craters. In *Physics and Astronomy of the Moon*, ed. Z. Kopal, pp. 283–359. New York: Academic
Shoemaker, E. M. 1963.. Impact mechanics at Meteor Crater, Arizona. In *The Moon, Meteorites and Comets*, ed. B. M. Middlehurst, G. P. Kuiper, pp. 301–6, Chicago: Univ. Chicago Press
Taylor G. I. 1950. The formation of a blast wave by a very intense explosion: II. The atomic explosion of 1945. *Proc. R. Soc. London Ser. A* 201: 175–86
Worthington, A. M. 1908. *A Study of Splashes.* London: Longmans & Green
Worthington, A. M., Cole, R. S. 1897. Impact with a liquid surface, studied by the aid of instantaneous photography. *Philos. Trans. R. Soc. London Ser. A* 193: 137–48